

Analysis of the influence of module construction upon forward osmosis performance

Robert W Field^{*1}, Farrukh Arsalan Siddiqui^{1, 4}, Pancy Ang³, Jun Jie Wu²

¹ University of Oxford, Department of Engineering Science, United Kingdom

² Durham University, School of Engineering and Computing Sciences, United Kingdom

³ School of Civil and Environmental Engineering, Nanyang Technological University, Singapore

⁴ Bahauddin Zakariya University, Department of Mechanical Engineering, Multan, Pakistan

Abstract

The potential of a commercial forward osmosis (FO) module to recover water from NEWater brine, an RO retentate, was assessed by taking an innovative approach to obtaining the mass transfer coefficients. The performance comparison of the spiral wound (S-W) FO module with that of the flat sheet laboratory unit suggests that the winding involved in S-W construction can adversely affect performance; the values for the S-W mass transfer coefficients were half of those expected. This first-of-its-kind performance comparison utilised coupons of the membrane and spacers taken from the module. The module was used both in the conventional manner for FO and in the reverse manner with the active layer facing the draw solution. Estimates of membrane parameters and mass transfer coefficients experiments for the two orientations were obtained using pure water, 10mM and 25mM NaCl solution on the feed side and 1M NaCl as draw solution. The fouling potential of NEWater brine *per se* was found to be low. These are the first results with a S-W module that suggest potential for this niche application; nevertheless the level of the water flux through the S-W module clearly indicates that industrial applications of S-W FO will be constrained to special cases.

Key words: forward osmosis; mass transfer; spiral wound; feed spacer; membrane deformation

Highlights:

Novel procedure for extracting mass transfer coefficients from FO data

Tightness of winding in spiral wound modules can adversely affect performance

Fouling potential of NEWater brine *per se* is low

In FO modules selection of appropriate spacing materials is crucial to performance

Necessity for improved channel hydrodynamics

1. Introduction

It is appropriate in an issue in honour of Professor Raphael Semiat that we should be analysing the influence of module construction upon overall performance. In this study the performance of a commercial spiral wound Forward Osmosis (S-W FO) module is compared with that of a bench-scale flat sheet unit incorporating membrane and spacers cut from the S-W FO module. A significant difference was found experimentally and explained through an analysis of mass transfer. We have noted with great interest a recent paper by Semiat and co-workers on an analysis of FO mass transfer resistances via CFD analysis and film theory [1]. In that paper the use of 2D finite element CFD model and the common film model (FM) were compared and it was concluded that the FM model overestimates the significance of the permeation resistance of the FO membrane support layer. As the present study is a comparative one between module types (S-W FO vs flat sheet laboratory unit) we have used the traditional approach for the analysis, especially as a CFD analysis has not been undertaken. However it is noted that Sagiv *et al's* [1] conclusions are in accord with our recent FM based study [2] and other CFD [3,4] ones in questioning the oft reported dominance of the contribution of the internal concentration polarisation (ICP) over that of external concentration polarisation (ECP). Contrary to popular wisdom some analyses [e.g. 1] suggests that improvements in FO water permeability are in part more likely to emerge from improved channel hydrodynamics (to decrease external concentration polarisation) rather than from more permeable and thinner membrane support layers. Here we compare the mass transfer characteristics of a S-W FO module with that of a standard flat sheet laboratory unit in order to assess the influence of construction upon performance.

At this stage it is customary in papers on FO to say that osmotically-driven membrane processes represented by (FO) and Pressure Retarded Osmosis (PRO), are emerging membrane technologies that show great promise to address the global challenges in water and energy supply. The paper may even continue, as in [5], to say with regard to PRO that “it did not achieve rapid advancement until the operation of the first prototype PRO osmotic power plant in Norway in 2008” and then completely fail to say that the Statkraft prototype (which was formally opened on 24 November 2009) was closed in 2014. Furthermore the facility had produced power at just 2-4 kW. It was reported that the Norwegian power company Statkraft had shelved its efforts because the technology could not be sufficiently developed within the current market outlook to become competitive “within the foreseeable future” [6].

The outlook for osmotically driven processes is not as rosy as generally portrayed. Firstly it is widely recognised that the water flux in an osmotically driven process is severely limited by “concentration polarisation” [2,7] which arises either by dilution of the high-osmotic-pressure draw solution (FO mode) or undesirable concentration of the feed solution inside the FO support structure (PRO mode). Secondly there are challenges in designing compact modules [2,8] and as noted above ECP can also cause a very significant constraint. Due to this, two of the current authors have expressed strong doubts as to whether forward osmosis will ever successfully compete with reverse osmosis for desalination of seawater because of inherent mass transfer limitations [2]. From a solid theoretical analysis it was concluded that the future of forward osmosis probably lies with niche applications of very high salinity brines [2]. It is now generally accepted that FO will not compete with reverse osmosis for desalination of seawater and that if FO has a widespread future beyond niche applications it will involve the brine from traditional RO plants acting as the draw solution. The potential of recovering water from NEWater brine, currently a reject stream, will be discussed at the end of the paper in section 4.

As noted by others [9] numerous academic groups around the world have made new membranes for forward osmosis but at full-scale production the dominant platform has been a cellulose acetate membrane from Hydration Technology Innovations (HTI). Whilst [9] reported on a newly launched forward osmosis membrane from HTI, namely their thin film composite (TFC) membrane, our study was based on their traditional cellulose acetate membrane.

2. Materials and Methods

2.1 Chemicals and membranes

Unless otherwise specified, all the chemicals used in this study are ACS grade and all the solutions were prepared using ultrapure water with a resistivity of $18.2\text{M}\Omega\text{ cm}$ produced by a Mill-Q system (Millipore Integral 10 Water Purification System). In all experiments 1M NaCl was used as draw solution. For the work at pilot scale, tap water was used in the preparation of the draw solution. The NEWater brine was delivered in 25L carboys.

The osmotic membrane used in this study was a commercial FO membrane, FO Spiral Elements SeptraMem 4040 FO Standard Spacer by Hydration Technologies, Inc. (HTI, Albany, OR). It is shown in Figure 1. This membrane has an asymmetric structure and is prepared by coating cellulose triacetate (CTA) into a polyester mesh [10]. It has been reported that the membrane itself has a thickness of less than $50\text{ }\mu\text{m}$ [11].



Figure 1 Cross-sectional view of the spiral wound CTA membrane taken out of its module casing (left) and unwound (right)

The dimensions of the module element are given in Figure 2. This diagram has been drawn for PRO mode i.e. AL-DS orientation. The spacer on the draw side was 0.87mm thick. The one on the feed side was 0.64mm thick and was in two pieces reflecting the fact that there is a central seal over 70 cm of the element – see Figure 1 (right) and Figure 2. The mesh sizes are also different as shown in Figure 3.

2.2 Pilot-scale set up and experiment

The feed solution (FS) and the draw solution (DS) were re-circulated, without concentration correction. Draw solution from the draw tank was pumped into the membrane element through a booster pump (BP), whilst a low pressure pump (LP) was used for the feed. Both pumps could have been low pressure pumps for the current work because in FO $\Delta p \sim 0$ but the rig had been designed to enable PRO operation as well as FO operation. The pumps were operated using computer control. A schematic of the layout is given in Figure 4. **More details can be found in [19].**

DS and FS tanks initially contained 100L of 1M NaCl solution and 100L of 25mM NaCl solution respectively at the start of the baseline tests. Subsequently the tests involved 100L of 1M NaCl solution

and 100L of NEWater brine. The NEWater brine solution is a retentate of sewage waste water that has been treated through dual membrane processes, firstly microfiltration and then reverse osmosis. The waste water that is not recycled for re-use is the retentate brine from the RO stage; the permeate from the RO stage is then UV treated. NEWater Brine was collected from a NEWater factory in Singapore. The 25mM NaCl solution was used for the baseline tests because it has similar conductivity to NEWater brine. Tap water was used for dilution of the NaCl solutions. All tests started with the DS and FS tanks containing 100L at appropriate concentrations.

During the runs, which were of 4 hours duration, the feed solution gradually became concentrated as a result of permeation of water from feed side to the draw side. This also resulted in dilution of the draw solution. By noting the conductivity values of solutions on both sides at the start and end of each run, the change in osmotic pressure difference could be estimated. Before moving to the next run, both solutions were adjusted to approximate levels. For the feed solution, tap water was added to the feed solution up to the level of the previous run and for the draw solution, 5 M NaCl was added as required until the conductivity of the draw solution matched that of 1 M NaCl solution. When analysing the results the mean concentrations during the 4 hour runs were used to calculate the overall driving force as the change in concentrations were modest being around 15%.

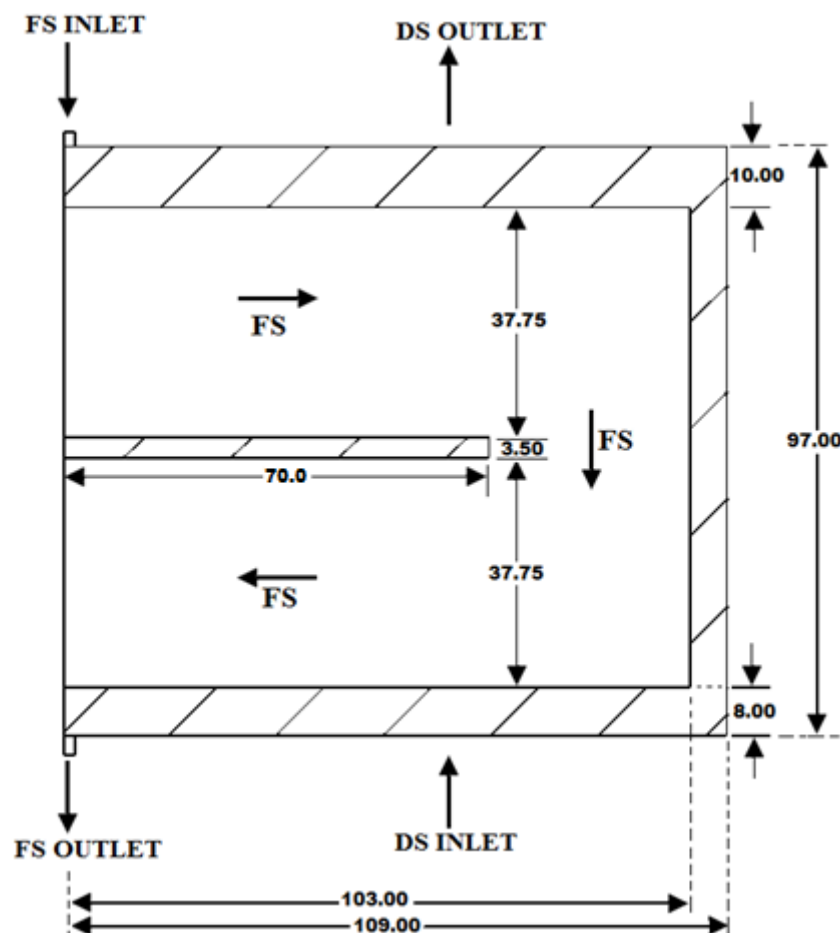


Figure 2 Dimensions (in cm) of pilot scale spiral wound CTA membrane element. The module was used both in the conventional manner for FO and in the reverse manner; the diagram has been drawn for the reverse arrangement i.e. AL-DS. In this arrangement the draw flows axially through the module whilst the feed flows within the envelope firstly spiralling out and then spiralling inwards.

The six runs with NEWater brine reported here were alternated between the AL-DS orientation and the AL-FS orientation. The orientation was reversed by simply interchanging the feed and draw tubings connecting the FS and DS tanks to the module. Before switching, the draw side was flushed thoroughly with tap water to remove any remaining salt.

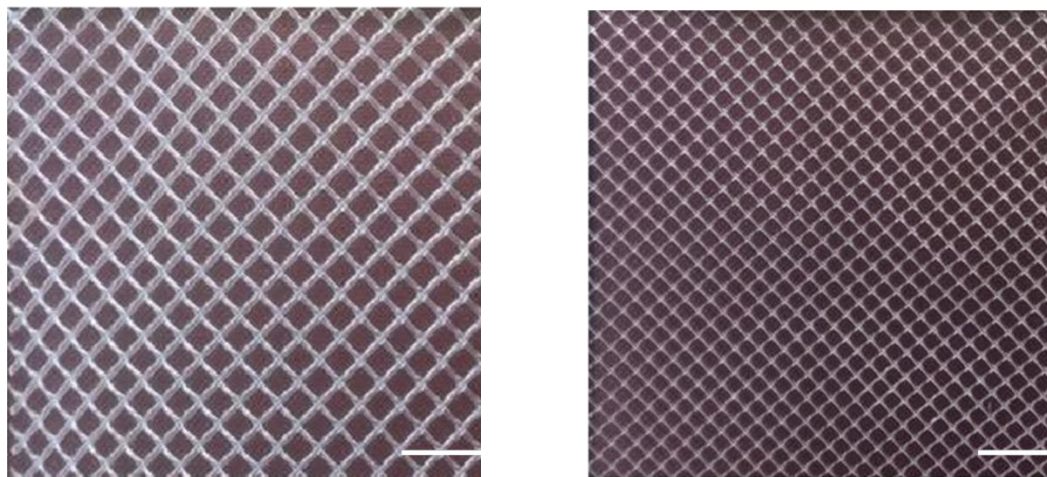


Figure 3 Photographs of the draw side (left) and feed side (right) spacers used within the spiral wound module. The scale bar is 10 mm

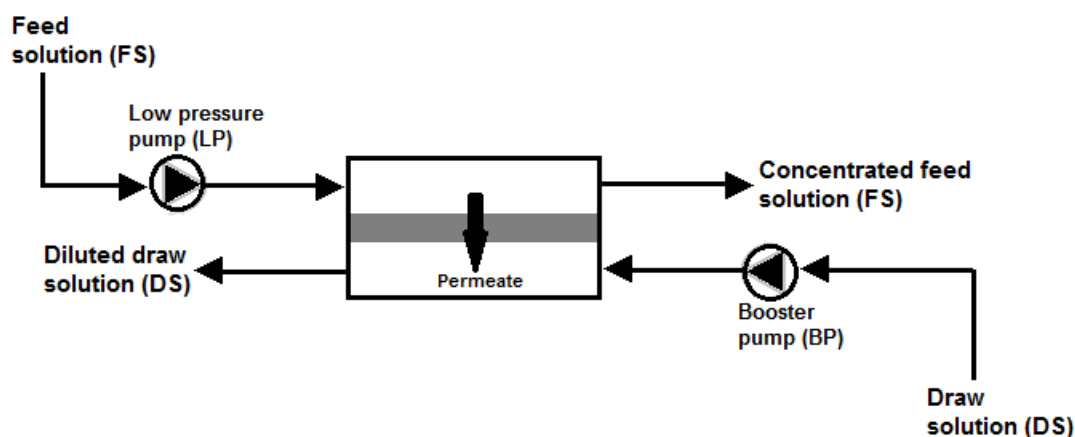


Figure 4 Schematic of the Pilot scale forward osmosis setup. The module had an effective membrane area of approximately 1.6 m².

2.3 Bench-scale set up and experiments

The bench-scale FO setup was essentially the same as that used elsewhere [12] except for the membrane cell which has identical channels on each side; the dimensions are a length 85mm and a cross-sectional flow area of 39 mm by 2.3 mm. These experiments used membrane coupons cut from the spiral wound modules and spacer material was also cut and placed in the channels but skins to ensure a tight fit were not used. (As noted in the later this may have been fortuitous.) The computer

controlled system with conductivity measurements and automatic dosing ensured that feed and draw concentrations remained constant. Two variable-speed peristaltic pumps were used to recirculate the respective feed and draw solutions at a flowrate of 0.4 L/min which gave a crossflow velocity of 0.074 m/s. The flow rates were not chosen to correspond to those used in the pilot scale set-up thus a classical mass transfer correlation was used to link the results from the two sets of experiments. The volumetric flux of water was determined at regular time intervals by measuring the mass changes of the feed tank; it was on a digital mass balance connected to a computer data logging system.

A limited number of reverse osmosis baseline experiments were conducted to obtain a second estimate of the 'A' parameter of the membrane. The maximum pressure used was 13.8 bar. A second method by which another estimate of 'A' could, in principle, be obtained is mentioned in section 3.2.

3. Results

3.1 Determination of water permeability and salt permeability coefficient

In the RO tests water flux increased linearly as the hydraulic pressure increased. The permeability was determined in the flat sheet laboratory unit to be 0.75 LMH per bar which gives an 'A' parameter of 2.08×10^{-12} m/s per Pa. This is close to the value of 1.87×10^{-12} m/s per Pa determined elsewhere [14] and comparable with the value of 3.3×10^{-12} m/s per Pa [13]. The value determined experimentally was used in all subsequent calculations.

From measurements of the conductivity before and after tests with the S-W module, and from knowledge of the starting and finishing volumes, the reverse salt flux was calculated for the seven sets of data available. This was then used to calculate values of 'B' parameter. The data for AL-DS and AL-FS were divided into two groups and equation (1) used to calculate 'B', given the 'A' value of 2.08×10^{-12} m/s per Pa.

$$\frac{B}{A} = \frac{J_s}{J_w} \beta RT \quad (1)$$

For AL-DS the 'B' value was 2.44×10^{-7} m/s but for AL-FS it was 1.88×10^{-7} m/s. These values are comparable with the value obtained using an RO set-up for the same membrane, namely 2.56×10^{-7} m/s (see entry CTA-HW in Table 3 of [13]).

3.2 Determination of mass transfer coefficients

The flux data obtained with the flat sheet laboratory unit for various saline solutions was used to determine the mass transfer coefficients. As the channel dimensions and crossflow velocities on either side were identical, and the variations of density and viscosity with salt concentration are minor, the Reynolds numbers for the two flows could be taken to be the same. The diffusivity of salt in water, D , has a moderate dependency upon concentration [15] and so allowance was made for this. Following some early work on spacer characterisation in spacer-filled channels [17] the Sherwood number was taken to be proportional to the Schmidt number raised to the power 0.33 thus the mass transfer coefficient in the channel was taken to vary with $D^{0.67}$. If the correlation in [14] were to have been used, the variation would have been taken to be $D^{0.60}$.

For the channel adjacent to the active layer the mass transfer coefficient is designated as k_c where subscript 'c' indicates channel. For the channel adjacent to the support layer the mass transfer coefficient is designated as k_{sup} where subscript 'sup' indicates the combined mass transfer coefficient for the support layer itself and the adjacent external mass transfer layer. The former can be written as D/S where D is the diffusivity of salt in water (it has a moderate dependency upon concentration [15])

and S is the structural parameter, defined as the product of the support layer thickness and tortuosity over its porosity [16]:

$$S = t \cdot \tau / \varepsilon \quad (2)$$

Thus

$$\frac{1}{k_{sup}} = \frac{1}{k_c} + \frac{S}{D} \quad (3)$$

For the AL-FS orientation, the equation relating flux, 'A', 'B' and the mass transfer coefficients k_c and k_{sup} can be written as:

$$J_w = A \left[\pi_{ds} \exp \left(-\frac{J_w}{k_{sup}} \right) - \pi_f \exp \left(\frac{J_w}{k_c} \right) \right] + B \left[\exp \left(-\frac{J_w}{k_{sup}} \right) - \exp \left(\frac{J_w}{k_c} \right) \right] \quad (4)$$

For the AL-DS orientation, the equation relating flux, 'A', 'B' and the mass transfer coefficients k_c and k_{sup} can be written as:

$$J_w = A \left[\pi_{ds} \exp \left(-\frac{J_w}{k_c} \right) - \pi_f \exp \left(\frac{J_w}{k_{sup}} \right) \right] + B \left[\exp \left(-\frac{J_w}{k_c} \right) - \exp \left(\frac{J_w}{k_{sup}} \right) \right] \quad (5)$$

These equations are fully consistent for those for FO found elsewhere e.g. [5] but are presented in a manner which avoids the use of an overall mass transfer coefficient. Furthermore it is readily seen that given (i) knowledge of fluxes and concentrations (and hence values of π_{ds} and π_f); (ii) estimates of the mass transfer coefficients k_c and k_{sup} and (iii) an estimate of the 'B' parameter then the 'A' parameter can be checked. The estimate of the 'B' parameter was constrained to be within 10% of the literature value cited above.

As is clear from equation (5), and the earlier work of Sagiv *et al* [1], estimation of the mass transfer coefficients depends on the permeability coefficients. For a given flux, overestimation of the RO derived coefficients 'A' and 'B' yields lower mass transfer coefficients and vice versa. Now it might be supposed that with sufficient data sets at various values of draw and feed salinities one could avoid the use of any RO derived coefficients and use just FO data to obtain estimates of coefficients 'A' and 'B' and the two mass transfer coefficients k_c and k_{sup} . In principle the number of data sets to hand was sufficient but given the uncertainties in the experimental data and the form of the equations, the variation in salinity was insufficient. Thus in common with others, the RO derived coefficients were used to inform the FO analysis.

For the FS laboratory unit there were six data sets and the fluxes were invariant with time when saline solutions were used as feed. The methodology for obtaining the best estimates of the two mass transfer coefficients was to change the values of k_c and k_{sup} (and 'B' within its constraint) until the six calculated values of 'A' found from equations (4) and (5) gave values of 'A' as close as possible to the set value of 2.08×10^{-12} m/s per Pa (i.e. 0.208 μ m/s per bar). The outcome is summarised in Table 1. We refer to "the two values of mass transfer coefficient" since there are two basic values and all other values could be linked to the base values by equation (6).

$$\frac{k}{k_0} = \left(\frac{D}{D_0} \right)^{2/3} \quad (6)$$

The values of mass transfer coefficients were independent of Reynolds number as it was invariant across these data sets. The $D^{0.67}$ allowance for the variation in diffusivity gave a maximum 5.4% correction in mass transfer coefficient.

Table 1 Data from Flat sheet laboratory and resultant mass transfers and structural parameter, S

Orientation	Feed salinity (mM)	Flux J_w $\mu\text{m/s}$	Estimated 'A' $\mu\text{m/s per bar}$	k_c $\mu\text{m/s}$	k_{sup} $\mu\text{m/s}$	S μm
AL-DS	0	6.28	0.228	14.1	3.5	321
AL-DS	10	5.53	0.205			
AL-DS	25	4.89	0.186			
AL-FS	0	3.81	0.229			
AL-FS	10	3.44	0.199			
AL-FS	25	3.31	0.195			

The value of 321 μm for the structural parameter is similar to that obtained by Tang *et al* [11] who gave a value of $\sim 400 \mu\text{m}$ but they made no allowance for external concentration polarisation (ECP) in their calculations. Their value was determined from RO experiments so the effect of ECP would have been only on one side.

The procedure for calculating the FO S-W module mass transfer coefficients k_c and k_{sup} was similar except that for the 'B' parameter the experimental values $2.44 \times 10^{-7} \text{ m/s}$ (AL-DS) and $1.88 \times 10^{-7} \text{ m/s}$ (AL-FS) were used. The results are summarised in Table 2. The estimated values are based upon an assumption that the structural parameter would be unchanged and that the mass transfer coefficients would scale with Reynolds number (based upon an empty channel) raised to the power of 0.33. The respective Reynolds numbers are 360 for the FS unit (both sides), 296 for the feed side of the S-W module and 108 for the draw side of the S-W module. Given that the spacers are a tight fit in the S-W unit, but unduly loose in the FS unit, the scaling is very approximate. At this stage it is noted the main significance lies with the experimental finding that the mass transfer coefficients in the S-W module are roughly half those found in the FS unit. This is discussed further in section 4.

Table 2 Analysis of results from Spiral-Wound module

	k_c $\mu\text{m/s}$	k_{sup} $\mu\text{m/s}$	S μm
Measured	6.66	1.71	645
Estimate for AL-FS based on FS unit using $Re^{0.33}$	13.2	3.11	321
Percentage of expected	50	55	200

3.3 Water recovery from NEWater brine - Flux variations with time

Both modules were used to assess the flux stability in FO operation when NEWater brine is the feed. Figure 5 shows a comparison with 25 mM NaCl, which is of similar salinity. This is for the flat sheet unit operated in AL-DS orientation and both feeds, but particularly the NEWater brine, foul the support structure at the fluxes generated.

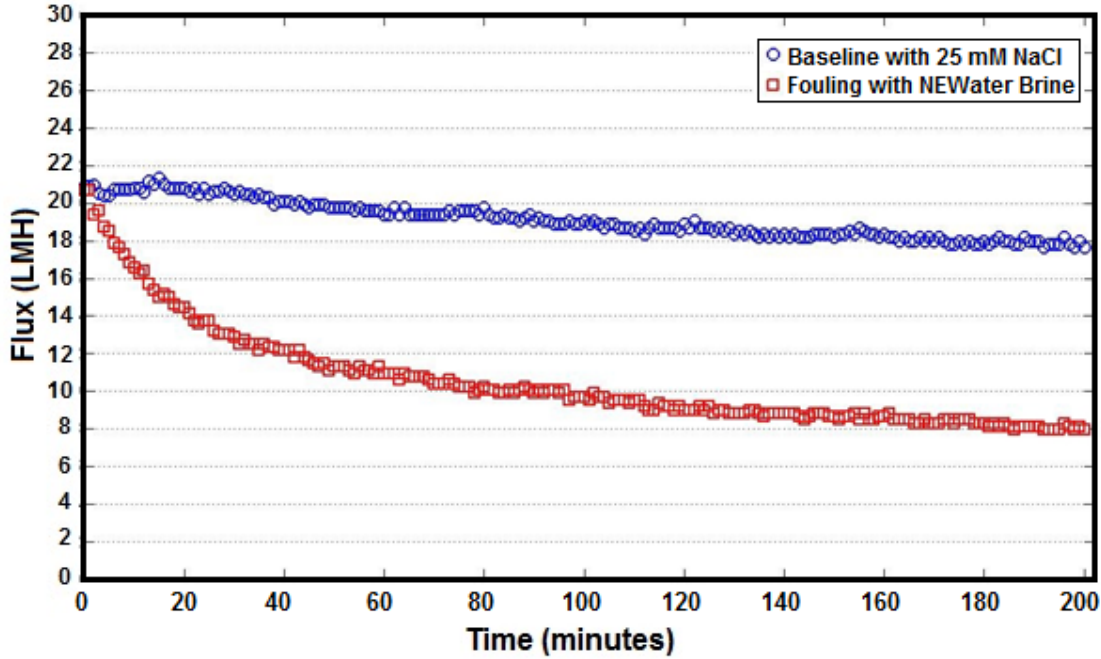


Figure 5: Flux vs Time for FO for fouling and base line tests with NEWater Brine and 25 mM NaCl solution at the feed side respectively and 1 M NaCl solution at draw side with flat sheet CTA membrane at bench scale (ALDS orientation)

When the flat sheet unit is operated in AL-FS orientation, flux becomes stable for both feeds (Figure 6). The run in AL-FS mode was preceded by one in AL-DS mode and the increase in flux for the NEWater brine over the first 30 minutes is attributed to the removal of accumulated fouling from the support structure; with the change in orientation the material in the support structure is now being washed out rather than convected inwards.

For the FO S-W module CTA membrane at pilot scale, a comparison (Figure 7) clearly showed that the AL-DS orientation out-performed that of AL-FS. This is counter intuitive because once allowance is made for the fact that there was no control of either the feed or the draw concentration, and that flux decline would occur due to a weakened driving force, the fouling in AL-DS mode was very modest or non-existent, but fouling was very apparent in AL-FS mode. This is seemingly in contrast to the result for the FS unit where the flux declined from 20 LMH to a plateau of around 8 LMH when the membrane was in AL-DS orientation. We have written 'seemingly' because one should distinguish between flux decline and the steady-state flux reached once any decline has occurred. We have concluded that the NEWater brine does not foul the support structure of the membrane when the fluxes are sufficiently low. There remains the question as to why, for the S-W module there is flux decline in AL-FS mode. An initial thought was, "Has the data been inadvertently swapped?"; however examination of the fluxes at the beginning of the runs shows that the fluxes for AL-FS orientation are lower than for AL-DS as one would expect; when the draw is on the same side as the support layer there is stronger internal concentration polarisation and fluxes are lower. Whilst this is expected, the fact that the fouling rates were higher for the AL-FS orientation was unexpected. The data shown is the mean for three runs but all of the individual flux declines with AL-FS were over 40%. In the discussion we consider an explanation.

For the S-W module the fact that the NEWater feed was in the channel adjacent to the support side did not lead to significant fouling when the flux was just 5 LMH. There are two key differences between the FS unit and S-W module, namely the volumetric flux and the tightness of the spacers. These factors are discussed further in section 4.

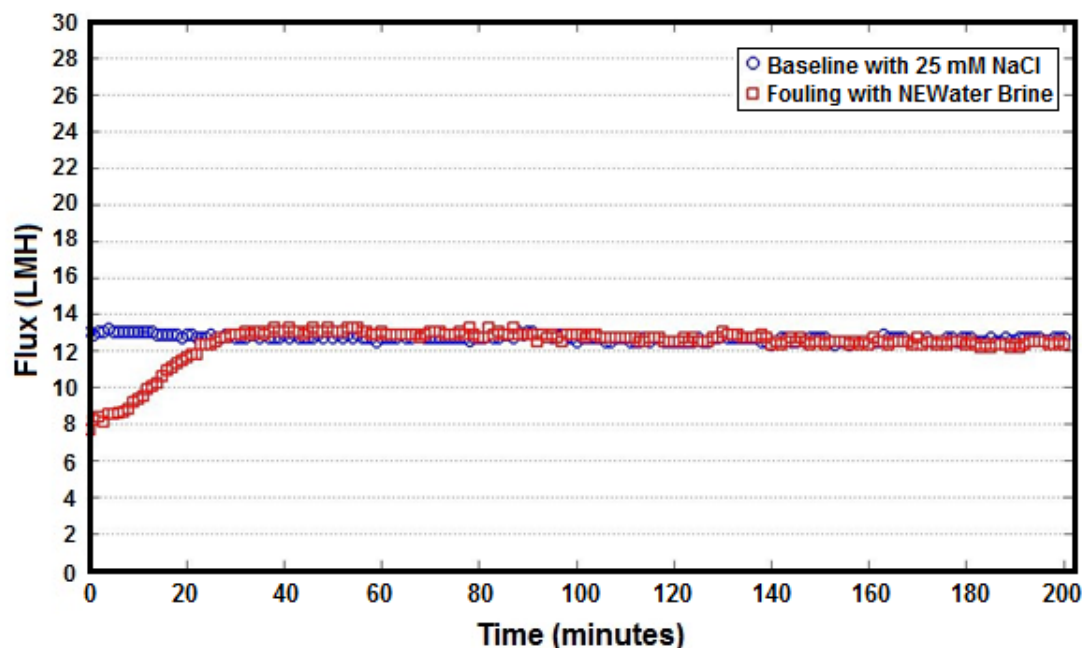


Figure 6: Flat sheet CTA membrane at bench scale run in ALFS orientation, operated under standard conditions, after having been run in ALDS orientation. Comparison of Flux vs Time curves for (a) NEWater Brine and (b) 25 mM NaCl solution. For (a) there is an increase in flux over the first 30 minutes as the fouling accumulated during the ALDS run is cleared.

4. Discussion

Firstly we address the results from the mass transfer analysis and then consider the fouling results. For the S-W module the value of $6.66 \mu\text{m/s}$ for the channel adjacent to the active layer superficially compares well with those obtained by Da Costa who evaluated a large range of spacers [17]. Figure 10 in Da Costa *et al* [17] gives values of $4\text{--}8 \mu\text{m/s}$ depending on the angle of the spacer but in that study dextran, which has a significantly lower diffusivity than salt, was used. Thus the magnitude of the mass transfer coefficients found for the S-W module herein might be considered to be surprisingly small.

One of our main results is to show that a comparison between the FS unit and the S-W module indicates that the calculated mass transfer coefficients in the module are only about 50% of the corresponding values in the FS unit. This experimental comparison was not made at the same crossflow velocity. Given that the spacers are turbulence promoters one might have expected increases in mass transfer coefficients as the Reynolds numbers were similar. However this was not the case. Now the local fluxes in the S-W module will be higher than those based on the superficial area because part of the membrane surface will be obscured at the points of contact between the spacer and the membrane. In FO units this affects the mass transfer on both sides of the membrane and increases the degree of concentration polarisation on both sides. The tightness of the winding will also influence the degree of “blinding” and the estimated value of ‘S’ at $645 \mu\text{m}$ (Table 2) may reflect the fact that the effective porosity has been reduced through blockage of some pores. As shown by equation (2) ‘S’ is inversely proportional to porosity so a decrease in the latter increases the former.

Not having had a close duplication of the hydrodynamic conditions between FS and S-W modules has generated results suggesting shown that the tightness of the binding in S-W modules is important. This is probably a particular strong effect for FO because of the important of mass transfer on both

sides of the membrane, and is worthy of further investigation.

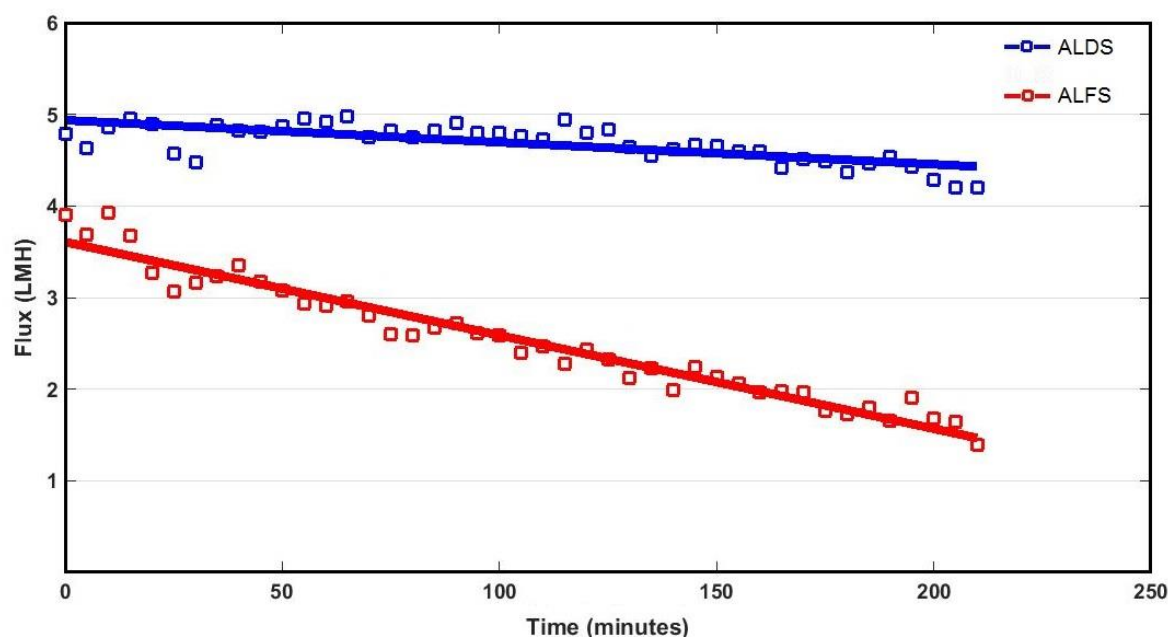


Figure 7: Spiral-wound CTA membrane at pilot scale - comparison AL-FS and AL-DS orientations. The flux-time profiles are for a feed of NEWater brine with a 1 M NaCl draw. There was no control of either the feed or the draw concentration and thus the driving force decreased with time; this is the reason for the slight decline in ALDS orientation. The data shown are the average of three runs.

The approach outlined in section 3.2 for the calculation of mass transfer coefficients will permit the mining of a wide range of data sets. Where the Reynolds numbers are different on each side the procedure will need to be generalised but this is straightforward. An analysis of the equations indicates that a wide range of feed solutions of different salinities should be used in order for accurate estimates of all parameters and coefficients to be obtained.

These are the first results for a S-W module to suggest that the potential application of recovering water from NEWater brine could be low fouling. In ALDS orientation the NEWater brine was found to hardly foul the support structure of the membrane albeit at the low flux of 5 LMH. Whilst with the laboratory FS rig there was fouling at an initial flux of 20 LMH (with flux declining to a steady-state value of 8 LMH), this fouling was readily reversible. It was established that reversal of the flow cleared the fouling within the support structure; see Figure 6 and comment in the caption. Thus at the low fluxes achieved in the S-W module the fouling potential of the NEWater brine is *per se* low. Whether these fluxes can lead to an economic process has yet to be established.

A key advantage of this potential application is that the draw solution would be brine from a seawater desalination plant which would be returned to that plant for recovery of the water extracted from the NEWater brine. Thus there would be no need to regenerate a draw solution and this is one of the new FO applications that might come to fruition. Much of the FO literature mistakenly equates the absence of high pressure pumps (as required by RO) with great potential for reducing energy requirements seemingly oblivious to the energy requirements of draw regeneration, which is generally required. The authors agree with one of the anonymous reviewers that the type of application is critical and that over-generalisation of the potential of FO should be avoided. FO has a place in the treatment of challenging waters, and potentially for special cases such as the present example, but realistic applications are not numerous.

Regarding the flux decline exhibited by NEWater brine there are four results overall, there being two orientations for both the FS unit and the S-W module. The AL-FS result for the FS unit indicates that the fouling potential of NEWater brine *per se* is very low indeed. In an essentially open channel, in AL-FS orientation, the critical flux [18] was not exceeded. With the S-W module there is essentially no fouling in AL-DS orientation. Here the draw flows across the more open less dense spacer (see Figure 3). Due to the mass transfer limitations only a low flux of *circa* 4.5 LMH was achieved but at this flux there was little fouling even though the NEWater brine was in the channel adjacent to the support structure.

However, with the S-W module there is fouling in AL-FS orientation but this is probably due to the fouling of the tight spacer (see Figure 3) by the draw solution. One might suppose that the NEWater brine would be more fouling than the draw solution but the results suggest that this was not the case. The NEWater brine that had passed through a microfiltration membrane during the NEWater process and which arrived in carboys was not diluted whereas the draw solution was prepared with tap water. In future pilot plant work the draw solution needs to be filtered to avoid the draw solution fouling the support layer and/or clogging the fine mesh. The unexpected fouling in the present work was readily reversible because the tests were run in alternate fashion and there was no discernible influence of an AL-FS run upon the next AL-DS run. Taken together the results suggest that with an appropriate spacer NEWater brine should be essentially non-fouling of a CTA membrane operated at an appropriate flux.

5. Conclusions

- (1) If osmotically driven processes are to play an increasing role, attention needs to be given to the necessity of improved channel hydrodynamics. The mass transfer coefficients in the Spiral-Wound module were around 50% lower than the corresponding values in the Flat Sheet unit and this severely limited the fluxes.
- (2) The fouling potential of NEWater brine *per se* is low but orientation and choice of spacer is crucial to performance. In an open channel in AL-FS orientation the critical flux was not exceeded.
- (3) Owing to the availability of a readily available saline stream, which does not require regeneration, recovering water from NEWater brine by FO may be economically feasible even though the fluxes are very modest.

Acknowledgements

FS gratefully acknowledges the financial support from the Higher Education Commission of Pakistan. FS is also grateful to SMTC at NTU, Singapore for hosting his year-long visit during which time the experimental data for this work was obtained, under the supervision of Dr She who also supervised Pancy Ang. RWF acknowledges useful discussions with Professor Tony Fane, and the essential analyses of JJW. All authors are grateful to PUB, Singapore for the provision of the NEWater brine.

References

1. A Sagiv, P.D. Christofides, Y. Cohen, R Semiat, On the analysis of FO mass transfer resistances via CFD analysis and film theory J Membr Sci 495 (2015) 198–205
2. R.W. Field, J.J. Wu, Mass transfer limitations in forward osmosis: are some potential applications overhyped? Desalination 318 (2013) 118–124
3. A. Sagiv, A. Zhu, P.D. Christofides, Y. Cohen, R. Semiat, Analysis of forward osmosis

- desalination via two-dimensional FEM model, *J. Membr. Sci.* 464 (2014) 161–172.
4. A. Sagiv, R. Semiat, Finite element analysis of forward osmosis process using NaCl solutions, *J. Membr. Sci.* 379 (2011) 86–96.
 5. Q. She, R. Wang, A.G. Fane, C.Y. Tang, Membrane fouling in osmotically driven membrane processes: A review *J. Membr. Sci.* 499 (2016) 201–233
 6. <http://www.powermag.com/statkraft-shelves-osmotic-power-project/> Accessed 31st May 2017
 7. C.Y. Tang, Q. She, W.C.L. Lay, R. Wang, R. Field, A.G. Fane, Modeling double-skinned FO membranes, *Desalination* 283 (2011) 178–186..
 8. B. Van der Bruggen and P. Luis, Forward osmosis: understanding the hype, *Rev Chem Eng* 31 (2014) 11-20. DOI 10.1515/revce-2014-0033.
 9. J. Ren, J.R. McCutcheon, A new commercial thin film composite membrane for forward osmosis, *Desalination* 343 (2014) 187-193
 10. T.Y. Cath, A.E. Childress, M. Elimelech, Forward osmosis: principles, applications, and recent developments, *Journal of Membrane Science* 281 (2006) 70–87.
 11. C.Y. Tang, Q. She, W.C.L. Lay, R. Wang, A.G. Fane, Coupled effects of internal concentration polarization and fouling on flux behavior of forward osmosis membranes during humic acid filtration, *J. Membr. Sci.* 354 (2010) 123–133
 12. Q. She, D. Hou, J. Liu, K.H. Tan, C.Y. Tang Effect of feed spacer induced membrane deformation on the performance of pressure retarded osmosis (PRO): Implications for PRO process operation, *J. Membr. Sci.* 445 (2013) 170-182
 13. J. Wei, C. Qiu, C.Y. Tang, R. Wang, A.G. Fane, Synthesis and characterization of flat-sheet thin film composite forward osmosis membranes, *J. Membr. Sci.* 372 (2011) 292-302
 14. A. Achilli, T.Y. Cath, A.E. Childress, Power generation with pressure retarded osmosis: An experimental and theoretical investigation *J. Membr. Sci.* 343 (2009) 42-52
 15. V. Vitagliano, P. A. Lyons, Diffusion Coefficients for Aqueous Solutions of Sodium Chloride and Barium Chloride *J. Am. Chem. Soc.* , 1956, 78 (18), 4538–4542. DOI: 10.1021/ja01599a008.
 16. S. Loeb, L. Titelman, E. Korngold, J. Freiman, Effect of porous support fabric on osmosis through a Loeb–Sourirajan type asymmetric membrane, *J. Membr. Sci.* 129 (1997) 243–249
 17. A.R. Da Costa, A.G. Fane, D.E. Wiley, Spacer characterization and pressure drop modelling in spacer-filled channels for ultrafiltration, *J. Membr. Sci.* 87 (1994) 79-98
 18. R.W. Field, D. Wu, J.A. Howell, B.B. Gupta, Critical flux concept for microfiltration fouling, *J. Membr. Sci.* 100 (1995) 259-272
 19. P. Ang, Evaluation of the Performance of Pressure Retarded Osmosis (PRO) Membrane Modules and Systems for Renewable Energy Recovery, *Env. Eng FYP Report in: School of Civil and Environmental Engineering, Nanyang Technological University, 2016.*